Journal of Environmental Management 233 (2019) 393–399

Contents lists available at ScienceDirect

Journal of Environmental Management

journal homepage: www.elsevier.com/locate/jenvman

Research article

Dissolved organic matter characterization of biochars produced from different feedstock materials

Anushka Upamali Rajapaksha[a,1], Yong Sik Ok[b,1], Ali El-Naggar[b,c], Hyojeon Kim[d], Fanhao Song[e], Seoktae Kang[d,**], Yiu Fai Tsang[f,*]

[a] Ecosphere Resilience Research Center, Faculty of Applied Sciences, University of Sri Jayewardenepura, Nugegoda, 10250, Sri Lanka
[b] Korea Biochar Research Center, O-Jeong Eco-Resilience Institute (OJERI) & Division of Environmental Science and Ecological Engineering, Korea University, Seoul 02841, Republic of Korea
[c] Department of Soil Sciences, Faculty of Agriculture, Ain Shams University, Cairo 11241, Egypt
[d] Department of Civil and Environmental Engineering, Korea Advanced Institute of Science and Technology (KAIST), Republic of Korea
[e] State Key Laboratory of Environmental Criteria and Risk Assessment, Chinese Research Academy of Environmental Sciences, Beijing, China
[f] Department of Science and Environmental Studies, The Education University of Hong Kong, Hong Kong

ARTICLE INFO

Keywords:
Biochar
PARAFAC
EEM spectra
Dissolved organic matter

ABSTRACT

Fluorescence excitation-emission matrix (EEM) spectroscopy coupled with parallel factor analysis (PARAFAC) enables better understanding of the nature of dissolved organic matter (DOM). In the current study, we characterized 10 biochar samples produced from different feedstocks using EEM/PARAFAC analysis. The composition and distribution of DOM substances present in biochar varied significantly according to feedstock, activation, and pyrolysis temperature. The integration of proximate and ultimate analyses of the solid phase together with water extractable organic matter (WEOM) phase of biochar provided new insights into the characterization of biochars, including nature and functionality. Characterization of both WEOM and solid phases is recommended for biochar research before large-scale production for various environmental and industrial applications.

1. Introduction

Biochar, a carbon-rich by-product produced by the incomplete combustion of biomass, has recently gained great interest for a variety of environmental applications (Lehmann and Joseph, 2009). Biochar can be used in the environment for carbon sequestration (El-Naggar et al., 2018a, 2018b; Kuzyakov et al., 2009; Matovic, 2011), immobilization of contaminants (Ahmad et al., 2014; Zhang et al., 2013), reduction of greenhouse gas emissions (Sethupathi et al., 2017; Woolf et al., 2010), improvement of soil fertility (Ding et al., 2016), and remediation of contaminated water and soil (El-Naggar et al., 2018c; Mayakaduwa et al., 2017; Rajapaksha et al., 2014, 2016). Being an emerging material that can be sustainably produced, interest in biochar research, including the comprehensive characterization of biochar samples, has quickly expanded.

The dissolved organic matter (DOM) content of biochars plays an important role in determining their application potential for environmental uses. However, release of DOM from biochars to the environment and the corresponding risk of contaminant transfer should be carefully considered when biochars are used as soil and water amendments because contaminants tend to attach to the DOM fraction of biochars (Wang et al., 2017). These processes affect microbial activities, carbon balance, and physiochemical properties of the ecosystems (Smith et al., 2016). However, little is known about the characteristics of soluble organic fraction of biochars (Jamieson et al., 2014; Lin et al., 2012; Uchimiya et al., 2013; Wu et al., 2018), and hence further investigations are warranted.

Fluorescence excitation-emission matrix (EEM) spectroscopy coupled with parallel factor analysis (PARAFAC) has been widely applied as a reliable technique to better understand the nature of DOM (Jamieson et al., 2014; Uchimiya et al., 2013). PARAFAC can be used to resolve the dominant fluorescent DOM components based on their excitation and emission (Ex/Em) maxima (Cuss and Guéguen, 2012; Ishii and Boyer, 2012). Various parameters of biochars, such as H/C and O/C

* Corresponding author.
** Corresponding author.
E-mail addresses: stkang@kaist.ac.kr (S. Kang), tsangyf@eduhk.hk (Y.F. Tsang).
[1] These authors contributed equally to this work and act as co-first authors.

https://doi.org/10.1016/j.jenvman.2018.12.069
Received 31 August 2018; Received in revised form 18 December 2018; Accepted 19 December 2018
Available online 24 December 2018

ratios, proximate contents, surface area, and pore volumes, are commonly used to correlate efficiencies of environmental applications (Ahmad et al., 2013; Sun et al., 2017). The importance of analyzing dissolved organic carbon (DOC) contents of biochars has been highlighted in previous studies (Jamieson et al., 2014; Lin et al., 2012; Uchimiya et al., 2013). Uchimiya et al. (2013) suggested the possibility of releasing DOC enriched with carboxyl and phenolic functionalities in biochars pyrolyzed at 350 °C − 500 °C. Moreover, Jamieson et al. (2014) observed clear differences in the behavior of DOM in biochars made from the same feedstock under different pyrolytic conditions. However, data on the integration of proximate and ultimate analyses of the solid phase together with water extractable organic matter phase (WEOM) of biochars are very limited. The effects of feedstocks and production conditions on the properties of DOM have not been fully understood. Thus, there is an urgent need to characterize the DOM of biochars due to its changes with biochar production conditions. In this study, ten biochar samples produced from different feedstocks were characterized using EEM/PARAFAC to evaluate feedstocks and production temperature dependencies on the compositional features of DOM. The variations in compositions and qualitative characteristics of DOM of biochars were also assessed using principal component analysis.

2. Materials and methods

2.1. Biochar production and characterization

Ten types of biochars derived from different feed stocks (i.e., soybean stover, garlic stem, rice husk, tea waste, perilla, wood pine chip, and oak wood) and produced under different conditions were used in this study. The powdered biomass samples were pyrolyzed at different temperatures (i.e., 300, 500, 400, and 700 °C) with a heating rate of 7 °C min^{-1} using a muffle furnace (N11/H Nabertherm, Lilienthal, Germany). To assure complete carbonization process, a holding time of 2 h was applied for each peak temperatures. For steam activation process, the pyrolyzed samples were treated with steam at a flow rate of 5 mL min^{-1} for 45 min, under the peak temperature (i.e., 300 or 700 °C). Korean Oak wood biochar produced at 400 °C was purchased from the Gangwon Charmsoot Company located in Hoengseong-gun, Gangwon Province, Korea.

2.1.1. Proximate analysis

The modified thermal analysis methods by McLaughlin et al. (2009) were used to calculate moisture, mobile matter, ash, and resident matter contents. Moisture content was determined by calculating the weight loss after heating the biochars at 105 °C for 24 h to a constant weight. Mobile matter (analogous to volatile matter), which reflects the non-carbonized portion in biochars, was determined as the weight loss after heating in a covered crucible at 450 °C for 30 min. Ash content was also determined as the remaining residue after heating at 700 °C in an open-top crucible. The resident matter, representing the portion of the biochar that is not ash, was determined by the difference in moisture, mobile matter, and ash. Each sample was analyzed in duplicate.

2.1.2. Surface area and morphological analysis

Surface areas of biochars were measured from N_2 isotherms at 77 K using a gas sorption analyzer (NOVA-1200; Quantachrome Corp., Boynton Beach, FL, USA). The samples were degassed for 6 h under vacuum at 473 K prior to conducting adsorption measurements. The N_2 adsorbed per gram of biochars was plotted versus the relative vapor pressure (P/P_o) of N_2 ranging from 0.02 to 0.2, and the data were fitted to the Brunauer–Emmett–Teller (BET) equation to calculate the surface area. Total pore volume was estimated from N_2 adsorption at P/P_o ~0.5. The Barrett–Joyner–Halenda method was used to determine the pore size distribution from the N_2 desorption isotherms (Park and Komarneni, 1998).

2.1.3. Elemental analyses

The elemental composition of biochars, including C, H, N, S, and O, was determined by dry combustion using an elemental analyzer (EA1110, CE Instruments, Milan, Italy). The molar ratios of H/C, O/C, (O + N)/C, and (O + N + S)/C were calculated. The pH and electrical conductivity of each biochar were determined in a suspension of biochar tp deionized water (1:5; w:v) using a digital pH meter (Orion A211, Thermo Electron Corp., Waltham, MA, USA) and a conductivity meter (Orion 555A, Thermo Electron Corp., Waltham, MA, USA) based on Lou et al. (2016) and Li et al. (2013) methods, respectively. The suspension was shaken for 1 h before measurement.

2.2. Excitation-emission spectra of biochars and PARAFAC modeling

For the qualitative characterization of soluble organic matters from biochar samples, EEM was investigated. To solubilize organic matters in a biochar, 0.4 g of each biochar sample was mixed with 30 mL of deionized water and then gently tumbled in sonication bath (Watson, USA) at the power of 30 W for 1 h. Each mixture was then set on the table for 30 min to settle down biochar particulates, and the supernatant was filtered through 0.45 μm membrane filter (Millipore, USA). For the EEM analysis, each filtrate was either diluted or concentrated until the DOC concentration reached 1 mg L^{-1}.

The EEM of each organic solution from a biochar was generated by scanning emission spectra from 250 nm to 600 nm at 1 nm intervals, with 5 nm increments of the excitation wavelength from 220 nm to 400 nm using a fluorescence spectrophotometer (RF5301PC, Shimadzu, Japan). To standardize the fluorescence signal, the signal was prepared from ultra-pure water and compared with sample signal at the Rayleigh scattering region as suggested Chen et al. (2003). The obtained EEM data were used in PARAFAC modeling using the DOMFluor (version 1.7) toolbox in MATLAB 7.6 (MathWorks, Natick, MA, USA). The effects of scatter lines of the EEMs were minimized by utilizing several important preprocessing steps: 1) the EEM of the ultra-pure water blank was subtracted from each sample's EEM; 2) a series of zero values was inserted in the region of no fluorescence (Ex≪Em) for the sample EEMs; 3) the residual Rayleigh and Raman scatters were regulated using interpolation methods derived from Bahram et al. (2006). The two-to seven-component model in PARAFAC was utilized to analyze for the samples' EEMs. Ex and Em loadings were constrained non-negative values and the residual analysis and split half analysis were used as indicators to identify the appropriate numbers of individual PARAFAC components (He et al., 2016). The maximum fluorescence intensities (Fmax) were used to assess the relative concentration of each PARAFAC component (Yu et al., 2015).

2.3. Statistical analysis

The statistical analyses were performed using IBM SPSS Statistics 23 (NY, USA). The values were tested by Pearson and Spearman's correlation coefficient (r) at significance levels of 0.01 and 0.05. The regression equations and the coefficients of determination (R^2) were carried out using OriginPro9.1 b215 (Origin Lab Corporation, Northampton, USA).

3. Results and discussion

3.1. Proximate and ultimate analysis, and elemental composition and surface functional group analysis of biochar samples

Table 1 summarizes the chemical and physical characteristics of biochars. All the biochars were in the alkaline pH range due to separation of alkali salts from the organic matrix in the feedstocks (Shinogi and Kanri, 2003). Ash content ranged from 5.03% to 45.62% in different biochars depending on feedstock types and production temperatures. The increase in production temperature resulted in high

Table 1
Proximate and ultimate analyses and physiochemical properties of biochars.

Sample	Proximate Analysis							
	pH	DOC (mg L^{-1})	Yield (%)	Moisture (%)	Mobile matter (%)	Resident matter (%)	Ash (%)	Reference
Soybean stover BC300	7.27	140.0	37.03 ± 0.48	4.50 ± 0.36	46.34 ± 2.99	38.75 ± 3.15	10.41 ± 0.52	Ahmad et al. (2012)
Soybean stover BC700	11.32	64.4	21.59 ± 2.47	0.42 ± 0.01	14.66 ± 1.68	67.74 ± 1.92	17.18 ± 0.25	Ahmad et al. (2012)
Oak wood BC400	10.17	14.6	–	6.83	31.42	56.04	5.03	Ahmad et al. (2013)
Rice husk BC700	9.87	1.6	33.38	3.42	26.13	31.21	39.24	Mayakaduwa et al. (2017)
Steam activated rice husk BC700	10.12	0.7	–	3.03	15.96	35.39	45.62	Mayakaduwa et al. (2017)
Steam activated tea waste BC700	10.48	0.4	18.42 ± 0.32	1.40 ± 0.48	18.62 ± 3.92	63.23 ± 3.29	16.73 ± 0.14	Rajapaksha et al. (2014)
Perilla BC700	10.62	219.0	23.36	0.08	6.46	51.56	41.89	Sethupathi et al. (2017)
Wood pine chip BC500	9.96	11.3	–	9.70	16.62	35.94	37.74	This study
Garlic stem BC300	–	658.7	–	–	–	–	–	This study
Garlic stem BC700	–	35.4	–	0.47	7.73	48.73	43.07	This study

Sample	Ultimate analysis											
	[a]C (%)	[a]H (%)	[a]N (%)	[a]O (%)	[a]S (%)	Molar H/C	Molar O/C	Molar [(O+N)/C]	Surface area (m^2 g^{-1})	Pore volume (cm^3 g^{-1})	Pore diameter (nm)	Reference
Soybean stover BC300	68.81	4.29	1.88	24.99	0.04	0.74	0.27	0.30	5.61	–	–	Ahmad et al. (2012)
Soybean stover BC700	81.98	1.27	1.30	15.45	0.00	0.19	0.14	0.16	420.30	0.19	–	Ahmad et al. (2012)
Oak wood BC400	88.71	1.21	0.36	9.72	–	0.16	0.08	–	270.76	0.12	1.10	Ahmad et al. (2013)
Rice husk BC700	50.56	1.29	0.65	7.67	–	0.32	0.12	–	236.74	0.05	5.29	Mayakaduwa et al. (2017)
Steam activated rice husk BC700	–	–	–	–	–	–	–	–	251.47	0.08	4.86	Mayakaduwa et al. (2017)
Steam activated tea waste BC700	82.37	2.06	3.89	11.57	0.10	0.299	0.10	0.15	576.09	0.1091	1.99	Rajapaksha et al. (2014)
Perilla BC700	71.83	0.91	1.46	15.27	0.12	0.15	0.16	–	473.39	0.07	3.43	Sethupathi et al. (2017)
Wood pine chip BC500	89.22	2.67	0.20	7.90	0.01	0.36	0.07	–	324.61	–	–	This study
Garlic stem BC300	58.94	4.81	1.47	34.57	0.20	0.97	0.44	0.46	1.49	–	–	This study
Garlic stem BC700	63.88	1.49	1.32	32.60	0.71	0.28	0.38	0.40	201.72	0.037	5.17	This study

[a] Ash and moisture free.

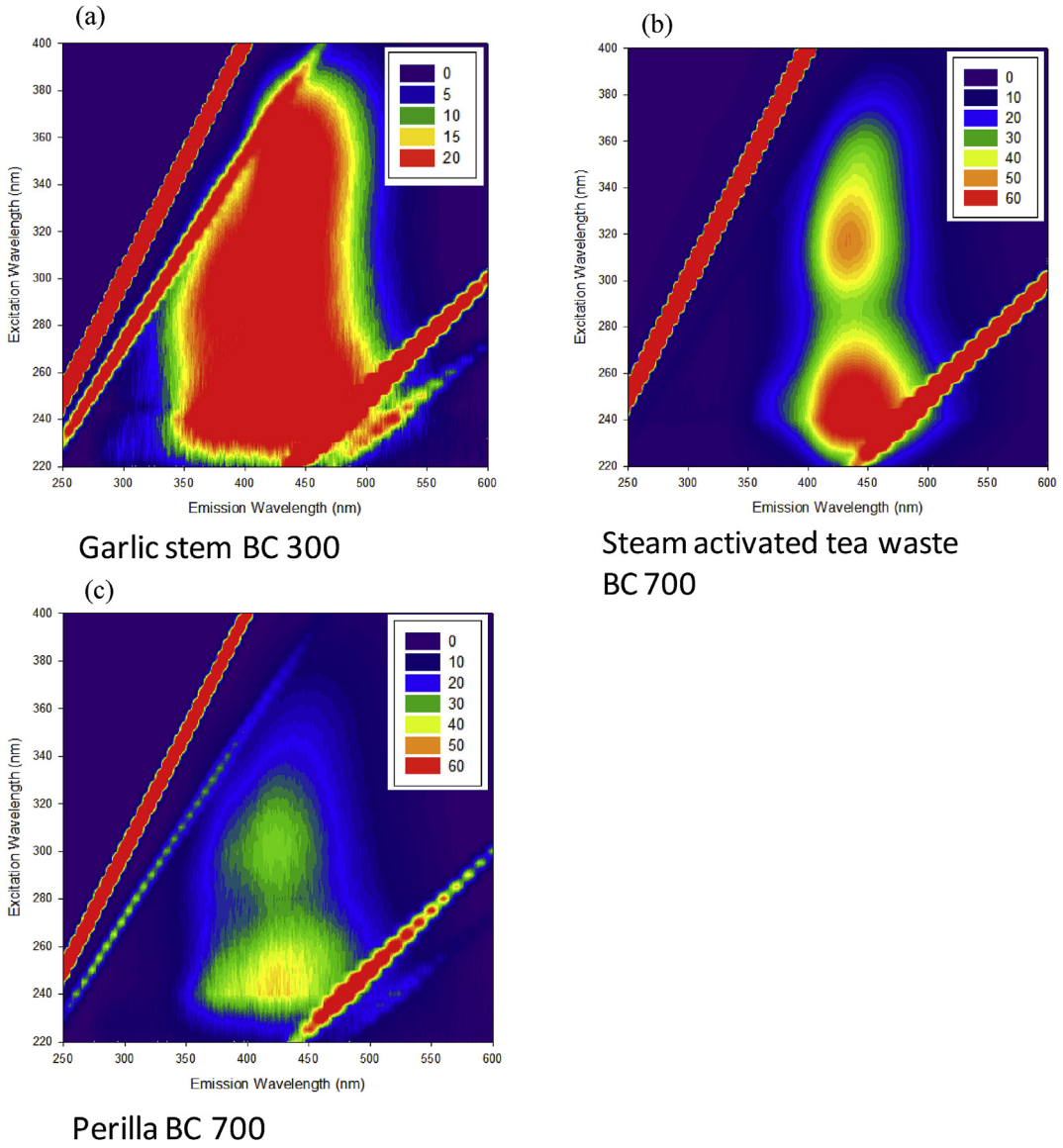

Fig. 1. Fluorescence EEMs of biochar samples. (a) Garlic stem BC300 (300 °C), (b) Steam activated tea waste biochar BC700 (700 °C), (c) Perilla BC700 (700 °C).

ash content due to the concentrations of minerals and organic matter combustion residues (Ahmad et al., 2012; Cao and Harris, 2010). The surface areas of biochars produced at 700 °C (i.e., soybean stover BC700: 420.30; garlic stem BC700: 201.72) were extremely high compared with that of biochars produced at 300 °C (i.e., soybean stover BC300: 5.61; garlic stem BC300: 1.49). This is due to the removal of volatile materials, thereby increasing the pore volumes of biochars (Ahmad et al., 2012). The low molar ratios of H/C indicated that biochars produced at high temperature (e.g., 700 °C) are highly carbonized than those produced at low temperature (e.g., 300 °C and 400 °C). Moreover, the relatively low O/C ratio values of biochars produced at 700 °C indicated that they are less hydrophilic compared with those produced at 300 °C and 400 °C.

The surface functional groups analysis using Fourier-transform infrared spectroscopy (FTIR) have confirmed the highly aromatic nature of high temperature produced biochars (Ahmad et al., 2012; Mayakaduwa et al., 2017; Rajapaksha et al., 2014). The biochars produced at 300 °C (i.e., soybean stover BC300, tea waste BC300, and garlic stem BC300) showed the bands at the region from 3200 to 3500 cm^{-1}, which correspond to the stretching vibration of the –OH group of bonded water and bands at the region from 2820 to 2980 cm^{-1}, which corresponds to aliphatic $–CH_2$ stretching variations (Ahmad et al., 2012; Rajapaksha et al., 2014). These peaks were noticeably decreased in biochars produced under high temperature, indicating the loss in labile aliphatic compounds. However, comparison of steam activated biochars with non-activated biochars produced under same temperature indicated that surface functional groups were almost same. Physical activation process under same temperature showed lack of significant changes of surface functional groups (Rajapaksha et al., 2014).

3.2. Fluorescent components identified by EEM-PARAFAC modeling

The EEMs of different biochar samples showed various fluorescence characteristics and provided for compositions associated with humic-like, fulvic-like, and protein-like substances (Fig. 1 and Fig. S1). The fluorescence EEM data were applied to PARAFAC modeling to distinguish the various fluorescent components in all biochar samples based on their origins (Figs. 2 and 3). EEM-PARAFAC identified four fluorescent components (i.e., C1 - C4). Component 1 (C1), which assigned as a UVA humic-like component, had a primary and a secondary peak at 340/430 nm (Ex/Em) and 260/430 nm (Ex/Em), respectively. Component 2 (C2), which assigned as a protein-/tannin-like component, exhibited two maxima at 220/370 nm (Ex/Em) and 280/370 nm (Ex/Em).

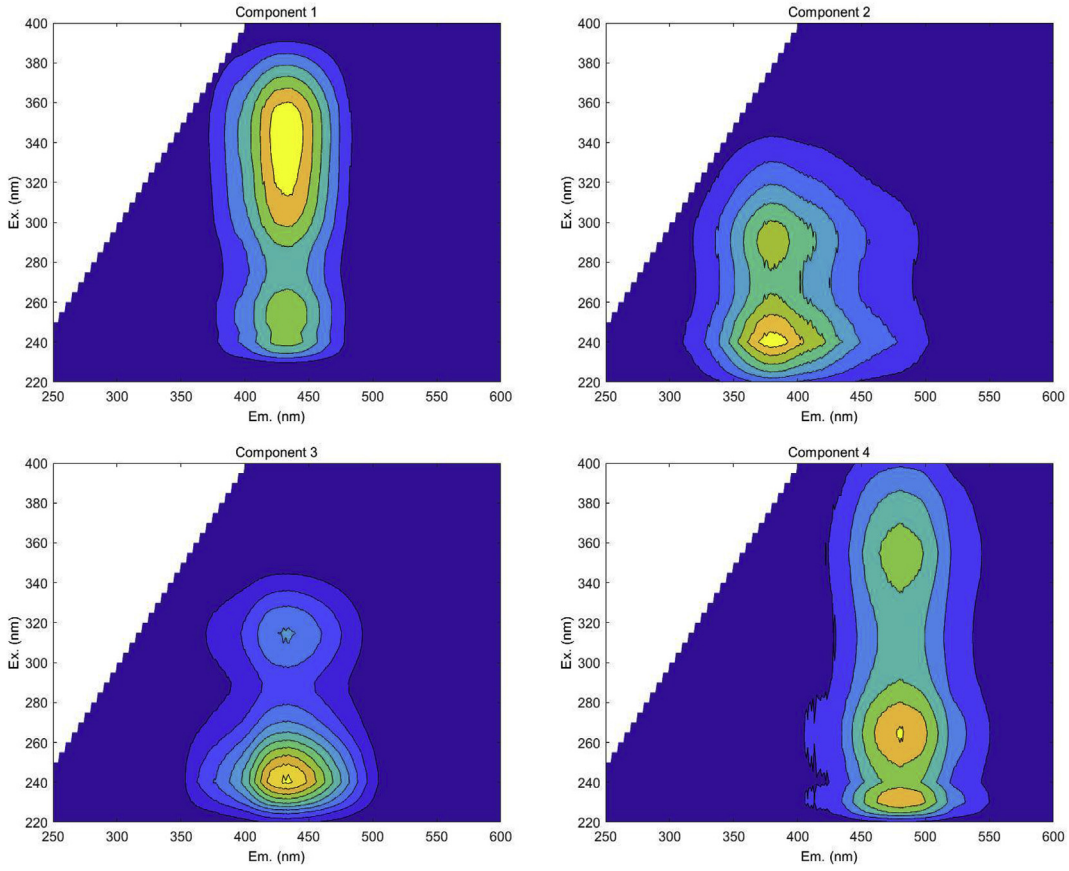

Fig. 2. Deconvoluted PARAFAC components.

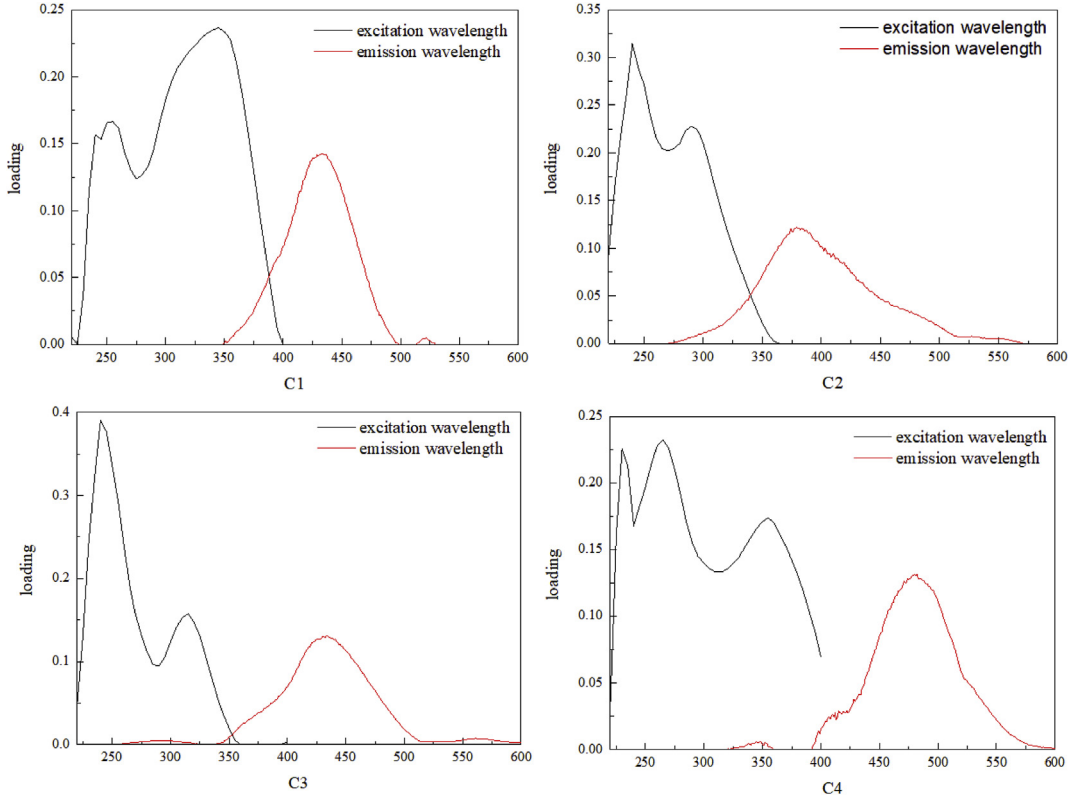

Fig. 3. Ex/Em loading of deconvoluted PARAFAC components (C1- C4).

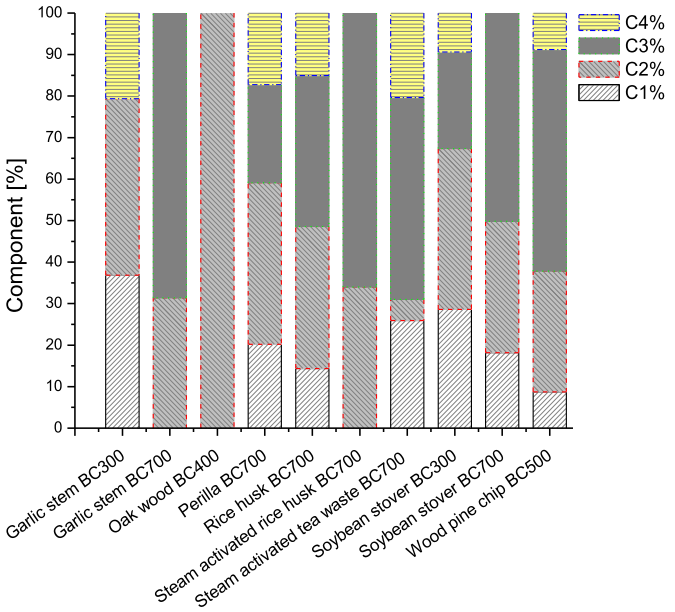

Fig. 4. Distribution of PARAFAC components (C1: UVA humic-like component, C2: protein/tannin-like component, C3: fulvic acid-like component, C4: terrestrial humic-like component) of different biochar samples (GS 300: Garlic stem BC300, GS 700: Garlic stem BC700, OW400: oak wood BC400, PE 700: Perilla BC700, RH 700: Rice husk BC700, SA-RH 700: Steam activated rice husk BC700, SA-TW 700: Steam activated tea waste BC700, SS 300: Soybean stover BC300, SS 700: Soybean stover BC700, WP 500: Wood pine chip BC500).

Table 2
Exponential regression analysis of PARAFAC components (i.e., C1, C2, C3, C4) and DOC and pH of different biochar samples.

Element	Equation	R^2	*P*	n
DOC				
C1%	$Y = 8.6 + 0.08X\text{-}7.1E\text{-}5X^2$	0.40	< 0.01	10
C2%	$Y = 37.5 + 0.012X\text{-}6.83X^2$	−0.02	ns	10
C3%	$Y = 47.2\text{-}0.12X + 7.9E\text{-}5X^2$	0.20	< 0.05	10
C4%	$Y = 6.6 + 0.02X\text{-}1.96X^2$	0.06	< 0.005	10
pH				
C1%	$Y = 5.3 + 0.67X\text{-}0.02X^2$	0.20	< 0.05	10
C2%	$Y = 10.6\text{-}0.10X + 9.87E\text{-}4X^2$	−0.31	< 0.05	10
C3%	$Y = 8.5 + 0.2X\text{-}0.004X^2$	0.35	< 0.01	10
C4%	$Y = 7.31 + 0.15X + 8.8X^2$	−0.19	< 0.05	10

DOC = dissolved organic carbon; ns = non-significant.

This result indicates the presence of tryptophan and/or phenolic-like substances. Component 3 (C3) that assigned as a fulvic acid-like component showed a maximum peak at 260/440. Component 4 (C4) that assigned as a terrestrial humic-like component was found at extended Ex/Em of 270/490 nm and 350/490 nm.

3.3. Fluorescence characteristics of water extractable organic matter (WEOM)

The vast disparity in biochar production conditions and feedstocks led to a variance of WEOM characteristics among the different biochar samples. The highest relative abundance of humic-like substances (i.e., C1 and C4) was found at the garlic stem BC300 (37% and 21%, respectively). However, garlic stem biochars lost these humic substances under high pyrolysis temperature (i.e., 700 °C) (Fig. 4). A similar observation was found in soybean stover biochars. Soybean stover BC300 showed higher existence of humic substances, C1 and C4 (29% and 9%, respectively) than soybean stover BC700 (18% and 0%, respectively) in the WEOM phase. The high red-shifted Ex/Em maximum in both biochars (i.e., garlic stem BC300 and soybean stover BC300) demonstrates the high aromaticity and high molecular weight of those biochars (Fig. S1). However, the red-shifting of fluorescence emission did not appear with the same feedstock under higher pyrolysis temperature (i.e., 700 °C). The increased pyrolysis temperature could influence the relative contribution of PARAFAC components. The humic-like substances, consisting of (poly)phenolics and other aromatic structures, may decompose under high pyrolysis temperature. Therefore, the release of humic-like DOM substances may be enhanced under high pyrolysis temperature. These results indicate the vital role of pyrolysis temperature on DOM fraction characteristics in biochars. Steam activation appeared as another potential factor affecting the existence of humic-like substances in biochars. For instance, the steam activation of rice husk BC700 led to the loss of its humic-like substances (Fig. 4).

Humic-like substances in biochar samples reflect the existence of humification process into the biomass. Humification process occurs via the biodegradation of fresh organic matter by microorganisms (Zhang et al., 2014). This process converts lower molecular weight organic compounds in substances into higher molecular weight polymers and compounds. The existences of humic acid-like substances in some biochar samples reflect the stability of these biochar samples (Zhang et al., 2014).

The phenolic-like and fulvic-like substances have lower molecular weight and a higher degree of solubility than humic acid-like substances. The highest ratio of tryptophan and/or phenolic-like substances was recorded in oak wood BC400 (100%), where no other DOM components were detected (Fig. 4). The results from this study suggested that the feedstock affects the existence of protein-like components in biochars than other factors, such as pyrolysis temperature and activation. In term of fulvic-like components, they exhibited the opposite behavior with humic-like substances, as they increased under high pyrolysis temperature of the same feedstock compared with low pyrolysis temperature (Fig. 4).

3.4. Interactions of fluorescence components and biochar characteristics

Analysis of the solid and WEOM fractions was employed to elucidate the interactions between biochar properties and its DOM fractions. Protein-/tannin-like component (C2) was correlated with S% ($r = +0.81$, $P < 0.05$) in biochar samples, which could be attributed to the affinity of sulfur with protein substances (e.g., sulfur-containing proteins). Protein-/tannin-like component was also correlated with molar O/C ratio ($r = +0.81$, $P < 0.05$) in biochar samples. This relation indicates that the presence of tryptophan and/or phenolic-like groups increase with less carbonization ratio.

DOC had a positive correlation with the humic-like components, C1 ($r^2 = 0.4$) and C4 ($r^2 = 0.06$), in biochar samples (Table 2). On the other hand, DOC was negatively correlated with the fulvic-like component, C3 ($r^2 = 0.2$), while the relationship was not significant between DOC and C2. These results demonstrate that humic-like components in the WEOM phase of biochar are more dominant in biochar, which contain higher DOC in its solid phase.

The current study found some variations in the different biochar properties between both WEOM and solid phases. For instance, soybean stover BC300 showed lower carbon and aromatization levels than soybean stover BC700 in the solid phase (Table 1). However, soybean stover BC300 was observed to contain more humic-like components than soybean stover BC700 in the WEOM phase. This is in line with the results reported by Zhang et al. (2014). They detected a lack of humification substances in the WEOM phase of bamboo biochar sample; however, its solid phase had very high carbon content at high aromatization level. Based on this finding, we recommend the biochar characterization research to include the WEOM phase of biochar as well as its solid phase. In this aspect, the characterization of DOM using the EEM-PARAFAC modeling allows us to identify the biochar substances in the dissolved phase.

4. Conclusion

Four fluorescent components (i.e., C1: humic-like component, C2: protein-/tannin-like component, C3: fulvic acid-like component, C4: terrestrial humic-like component) were identified in different biochars using PARAFAC modeling. Pyrolysis temperature, activation, and feedstock were the major factors affecting the presence of different DOM substances. The abundance of protein-/tannin-like component in the WEOM phase of biochar was influenced mainly by feedstock and it was increased in biochar with less carbonization and higher sulfur content in the solid phase. Humic-like substances were affected mainly by biochar pyrolysis temperature and activation. On the other hand, fulvic-like component was affected by pyrolysis temperature and negatively correlated with the DOC. The results in this study suggested that the integration between the biochar characterization in WEOM and solid phases provides better understanding of biochar nature and functionality. EEM-PARAFAC modeling is recommended to use as a promising tool for the identification of different components in the dissolved phase of biochars.

Acknowledgements

This work was supported by the National Research Foundation of Korea (NRF) (No. NRF- 2015R1A2A2A11001432), the Korea Ministry of Environment as “Global Top Project” (No. 2016002100008), and the Research Grants Council of the Hong Kong SAR (No. 18202116).

Appendix A. Supplementary data

Supplementary data to this article can be found online at https://doi.org/10.1016/j.jenvman.2018.12.069.

References

Ahmad, M., Lee, S.S., Dou, X., Mohan, D., Sung, J.K., Yang, J.E., Ok, Y.S., 2012. Effects of pyrolysis temperature on soybean stover- and peanut shell-derived biochar properties and TCE adsorption in water. Bioresour. Technol. 118, 536–544.

Ahmad, M., Lee, S.S., Oh, S.E., Mohan, D., Moon, D.H., Lee, Y.H., Ok, Y.S., 2013. Modeling adsorption kinetics of trichloroethylene onto biochars derived from soybean stover and peanut shell wastes. Environ. Sci. Pollut. Res. 20, 8364–8373.

Ahmad, M., Rajapaksha, A.U., Lim, J.E., Zhang, M., Bolan, N., Mohan, D., Vithanage, M., Lee, S.S., Ok, Y.S., 2014. Biochar as a sorbent for contaminant management in soil and water: a review. Chemosphere 99, 19–23.

Bahram, M., Bro, R., Stedmon, C., Afkhami, A., 2006. Handling of Rayleigh and Raman scatter for PARAFAC modeling of fluorescence data using interpolation. J. Chemometr. 20, 99–105.

Cao, X., Harris, W., 2010. Properties of dairy-manure-derived biochar pertinent to its potential use in remediation. Bioresour. Technol. 101, 5222–5228.

Chen, W., Westerhoff, P., Leenheer, J.A., Booksh, K., 2003. Fluorescence Excitation−Emission matrix regional integration to quantify spectra for dissolved organic matter. Environ. Sci. Technol. 37, 5701–5710.

Cuss, C.W., Guéguen, C., 2012. Determination of relative molecular weights of fluorescent components in dissolved organic matter using asymmetrical flow field-flow fractionation and parallel factor analysis. Anal. Chim. Acta 733, 98–102.

Ding, Y., Liu, Y., Liu, S., Li, Z., Tan, X., Huang, X., Zeng, G., Zhou, L., Zheng, B., 2016. Biochar to improve soil fertility. A review. Agron. Sustain. Dev. 36, 36.

El-Naggar, A., Awad, Y.M., Tang, X.Y., Liu, C., Niazi, N.K., Jien, S.H., Tsang, D.C., Song, H., Ok, Y.S., Lee, S.S., 2018a. Biochar influences soil carbon pools and facilitates interactions with soil: a field investigation. Land Degrad. Dev. 29 (7), 2162–2171.

El-Naggar, A., Lee, S.S., Awad, Y.M., Yang, X., Ryu, C., Rizwan, M., Rinklebe, J., Tsang, D.C., Ok, Y.S., 2018b. Influence of soil properties and feedstocks on biochar potential for carbon mineralization and improvement of infertile soils. Geoderma 332, 100–108.

El-Naggar, A., Shaheen, S.M., Ok, Y.S., Rinklebe, J., 2018c. Biochar affects the dissolved and colloidal concentrations of Cd, Cu, Ni, and Zn and their phytoavailability and potential mobility in a mining soil under dynamic redox-conditions. Sci. Total Environ. 624, 1059–1071.

He, W., Lee, J.H., Hur, J., 2016. Anthropogenic signature of sediment organic matter probed by UV–Visible and fluorescence spectroscopy and the association with heavy metal enrichment. Chemosphere 150, 184–193.

Ishii, S.K.L., Boyer, T.H., 2012. Behavior of reoccurring PARAFAC components in fluorescent dissolved organic matter in natural and engineered systems: a critical review. Environ. Sci. Technol. 46, 2006–2017.

Jamieson, T., Sager, E., Guéguen, C., 2014. Characterization of biochar-derived dissolved organic matter using UV–visible absorption and excitation–emission fluorescence spectroscopies. Chemosphere 103, 197–204.

Kuzyakov, Y., Subbotina, I., Chen, H., Bogomolova, I., Xu, X., 2009. Black carbon decomposition and incorporation into soil microbial biomass estimated by ^{14}C labeling. Soil Biol. Biochem. 41, 210–219.

Lehmann, J., Joseph, S., 2009. Biochar for environmental management: an introduction. In: Lehmann, J., Joseph, S. (Eds.), Biochar for Environmental Management. Earthscan, London, pp. 1–12.

Li, X., Shen, Q., Zhang, D., Mei, X., Ran, W., Xu, Y., Yu, G., 2013. Functional groups determine biochar properties (pH and EC) as studied by two-dimensional ^{13}C NMR correlation spectroscopy. PLoS One 8, 65949.

Lin, Y., Munroe, P., Joseph, S., Henderson, R., Ziolkowski, A., 2012. Water extractable organic carbon in untreated and chemical treated biochars. Chemosphere 87, 151–157.

Lou, K., Rajapaksha, A.U., Ok, Y.S., Chang, S.X., 2016. Pyrolysis temperature and steam activation effects on sorption of phosphate on pine sawdust biochars in aqueous solutions. Chem. Speciat. Bioavailab. 28 (1–4), 42–50.

Matovic, D., 2011. Biochar as a viable carbon sequestration option: global and Canadian perspective. Energy 36, 2011–2016.

Mayakaduwa, S.S., Herath, I., Ok, Y.S., Mohan, D., Vithanage, M., 2017. Insights into aqueous carbofuran removal by modified and non-modified rice husk biochars. Environ. Sci. Pollut. Res. 24, 22755–22763.

McLaughlin, H., Anderson, P.S., Shields, F.E., Reed, T.B., 2009. All biochars are not created equal and how to tell them apart. In: Presented at: North American Biochars Conference, vols. 9–12 August, Boulder, CO., USA.

Park, M., Komarneni, S., 1998. Rapid synthesis of $AlPO_4$-11 and cloverite by microwavehydrothermal processing. Microporous Mesoporous Mater. 20, 39–44.

Rajapaksha, A.U., Chen, S.S., Tsang, D.C.W., Zhang, M., Vithanage, M., Mandal, S., Gao, B., Bolan, N.S., Ok, Y.S., 2016. Engineered/designer biochar for contaminant removal/immobilization from soil and water: potential and implication of biochar modification. Chemosphere 148, 276–291.

Rajapaksha, A.U., Vithanage, M., Zhang, M., Ahmad, M., Mohan, D., Chang, S.X., Ok, Y.S., 2014. Pyrolysis condition affected sulfamethazine sorption by tea waste biochars. Bioresour. Technol. 166, 303–308.

Sethupathi, S., Zhang, M., Rajapaksha, A., Lee, S., Mohamad Nor, N., Mohamed, A., Al-Wabel, M., Ok, Y.S., 2017. Biochars as potential adsorbers of CH_4, CO_2 and H_2S. Sustainability 9 (1), 121.

Shinogi, Y., Kanri, Y., 2003. Pyrolysis of plant, animal and human waste: physical and chemical characterization of the pyrolytic products. Bioresour. Technol. 90, 241–247.

Smith, C.R., Hatcher, P.G., Kumar, S., Lee, J.W., 2016. Investigation into the sources of biochar water-soluble organic compounds and their potential toxicity on aquatic microorganisms. ACS Sustain. Chem. Eng. 4, 2550–2558.

Sun, X., Shan, R., Li, X., Pan, J., Liu, X., Deng, R., Song, J., 2017. Characterization of 60 types of Chinese biomass waste and resultant biochars in terms of their candidacy for soil application. GCB Bioenergy 9, 1423–1435.

Uchimiya, M., Ohno, T., He, Z., 2013. Pyrolysis temperature-dependent release of dissolved organic carbon from plant, manure, and biorefinery wastes. J. Anal. Appl. Pyrol. 104, 84–94.

Wang, B., Zhang, W., Li, H., Fu, H., Qu, X., Zhu, D., 2017. Micropore clogging by leachable pyrogenic organic carbon: a new perspective on sorption irreversibility and kinetics of hydrophobic organic contaminants to black carbon. Environ. Pollut. 220, 1349–1358.

Woolf, D., Amonette, J.E., Street-Perrott, F.A., Lehmann, J., Joseph, S., 2010. Sustainable biochar to mitigate global climate change. Nat. Commun. 1, 56.

Wu, H., Dong, X., Liu, H., 2018. Evaluating fluorescent dissolved organic matter released from wetland-plant derived biochar: effects of extracting solutions. Chemosphere. https://doi.org/10.1016/j.chemosphere.2018.08.110.

Yu, H., Qu, F., Chang, H., Shao, S., Zou, X., Li, G., Liang, H., 2015. Understanding ultrafiltration membrane fouling by soluble microbial product and effluent organic matter using fluorescence excitation–emission matrix coupled with parallel factor analysis. Int. Biodeterior. Biodegrad. 102, 56–63.

Zhang, J., Lü, F., Luo, C., Shao, L., He, P., 2014. Humification characterization of biochar and its potential as a composting amendment. J. Environ. Sci. 26, 390–397.

Zhang, X., Wang, H., He, L., Lu, K., Sarmah, A., Li, J., Bolan, N.S., Pei, J., Huang, H., 2013. Using biochar for remediation of soils contaminated with heavy metals and organic pollutants. Environ. Sci. Pollut. Res. 20, 8472–8483.